TIME-SCALE CANONICAL MODEL FOR WIDEBAND SYSTEM CHARACTERIZATION

Ye Jiang and Antonia Papandreou-Suppappola

Dept. of Electrical Engineering, Arizona State University, Tempe, AZ 85287–7206

ABSTRACT

In this paper, we propose a time-scale canonical model as a discrete characterization of wideband linear time-varying systems. This representation decomposes a system output into discrete time shifts and Doppler scalings on the input, weighted by a smoothed discrete version of the wideband spreading function. We base this formulation on the Mellin transform that is matched to scalings. We also demonstrate that our proposed model inherently affords a joint multipath-scale diversity in wideband communication channels. By properly designing the signaling and reception schemes using wavelet techniques, we can achieve this diversity over a dyadic time-scale framework.

1. INTRODUCTION

Linear systems can be characterized in terms of their effect on the transmitted signal leading to discrete canonical representations that can be useful in many applications [**?**, **?**, **?**]. For example, the widely used tapped delay line model can effectively decompose the output of a linear system into a weighted summation of discrete time shifts. Thus, a frequency-selective channel can act as independent, flat fading channels yielding multipath diversity [?]. Similarly, the time-frequency canonical model based on the narrowband spreading function can decompose the output of a linear time-varying (LTV) system into a double weighted summation of discrete time and frequency shifts providing joint multipath-Doppler diversity [?]. Note that this time-frequency model is matched to narrowband system changes.

When the system changes are wideband, an important class of LTV systems is characterized by the wideband spreading function (WSF) to accurately account for Doppler scaling effects (compressions or dilations) [**?**]. Such systems are encountered in acoustic environments [?] and high-speed underwater communications [**?**]. However, no discrete implementations have been exploited yet to increase the performance of wideband systems.

In this paper, we propose a time-scale canonical model to decompose the WSF representation into a double weighted superposition of uniformly sampled time shifts and geometrically sampled Doppler scalings. We identify the Mellin transform and the Fourier transform as the matched tools to process the Doppler scalings and time shifts, respectively. We associate the sampling intervals with the signal's support in the Mellin and Fourier domains, and generate a finite expansion under realistic constrains on the wideband system's spread in the time-delay and scale planes. By properly designing the transmitted signal, our proposed model can be adapted to a dyadic time-scale sampling structure that enables the efficient use of wavelet techniques and ultimately leads to a time-scale RAKE receiver. We show by simulation that this receiver structure can provide multipath-scale diversity that can significantly increase the performance of wireless wideband systems.

The rest of the paper is organized as follows. Section 2 describes the WSF characterization. Section 3 discusses in detail the derivation of our proposed time-scale model. Section 4 demonstrates the achieved diversity gain via simulations over wideband communication channels.

2. WIDEBAND SPREADING FUNCTION REPRESENTATION

When a signal $x(t)$ is transmitted with a propagation speed c over a medium with wideband characteristics, it is transformed as $y(t) = \sqrt{|a|}\, x\left(a(t-\tau)\right)$, where $a \approx \frac{c+v}{c-v}$ is the Doppler scaling caused by a moving object with velocity v. In most real life applications, $|v| < c$, hence we will assume that $a > 0$. The propagation delay τ is due to reflections of $x(t)$ off scatterers in the medium.

A wideband LTV system can be considered as the result of fast moving scatterers that are continuously distributed in range and velocity [?]. The system output can thus be characterized by a superposition of the contributions from all scatterers as,

$$y(t) = \int_0^\infty \int_{-\infty}^\infty \chi(\tau, a)\sqrt{a}\, x\left(a(t-\tau)\right) d\tau da\,, \qquad (1)$$

where $\chi(\tau, a)$ is the WSF that indicates the strength of the scatter resulting in a time-delay τ and Doppler scaling a. Due to the physical restrictions on the system, $\chi(\tau, a)$ usually vanishes outside the regions of $[0, T_m]$ and $[A_0, A_1]$ in the time-delay and Doppler scaling domains, respectively.

*This work was supported by the NSF CAREER Award CCR-0134002.

When the system is randomly varying, $\chi(\tau, a)$ can be modeled as a stochastic process. A wideband scattering function (WSC) can be defined to measure the second-order statistics of the WSF. In particular, if the transmitted energy is scattered uncorrelatedly in the time-scale domain, then the WSC $\Omega(\tau, a)$ satisfies

$$E[\chi(\tau, a)\chi^*(\tau', a')] = \Omega(\tau, a)\delta(a - a')\delta(\tau - \tau') \qquad (2)$$

where $*$ denotes conjugation, E[$\cdot$] denotes expectation and $\delta(\cdot)$ is the Dirac delta function.

3. TIME-SCALE CANONICAL MODEL

In this section, we first review the Mellin transform that is needed for the transform-based approach of discretizing the time-scale parameters. After outlining the derivation of the time-scale canonical model, we provide a finite approximation for the resulting expansion model for systems with finite spreads. The detailed derivation is given in [**?**].

3.1. The Mellin transform

The Mellin transform (MT) of a functional $s(c)$ is [**?**]

$$\mathcal{M}_s(\beta) = \int_0^\infty \frac{1}{\sqrt{c}}\, s(c)\, \mathrm{e}^{j2\pi\beta \ln c} dc \qquad (3)$$

where c and β are dual Mellin variables. The inverse MT

$$s(c) = \int_{-\infty}^\infty \frac{1}{\sqrt{c}} \mathcal{M}_s(\beta) \mathrm{e}^{-j2\pi\beta \ln c} d\beta, \quad c > 0 \qquad (4)$$

decomposes $s(c)$ into a weighted expansion of hyperbolic functions. The MT is invariant (up to a phase shift) to scale changes in the same way that the Fourier transform is invariant to time shifts. Thus, the MT can be used to process scale changes in the same way that the Fourier transform handles time shifts [?, **?**].

The MT satisfies a multiplicative convolution property. More specifically, the MT of the *multiplicative convolution* of $s_1(c)$ and $s_2(c)$,

$$s(c) = s_1(c) \circledast s_2(c) = \int_0^\infty s_1(cz) s_2^*(z)\, dz\,,$$

is simply the product of their MTs,

$$\mathcal{M}_s(\beta) = \mathcal{M}_{s_1}(\beta)\mathcal{M}^*_{s_2}(\beta)\,. \qquad (5)$$

3.2. Discretization of the time-scale parameters

In order to derive the time-scale canonical representation, we first apply the multiplicative convolution property (5) and the inverse MT (4) to (1). For a causal signal $x(t)$, we obtain,

$$\begin{aligned} y(t) &= \int_{-\infty}^\infty \int_0^\infty (\chi^*(\tau, a)\sqrt{a})^* x\left(at_r\left(\frac{t-\tau}{t_r}\right)\right) da d\tau \\ &= \int_{-\infty}^\infty \int_{-\infty}^\infty \mathcal{M}^*_\theta(\beta;\tau)\mathcal{M}_g(\beta)\mathrm{e}^{-j2\pi\beta\ln\left(\frac{t-\tau}{t_r}\right)} \frac{d\beta d\tau}{\sqrt{\frac{t-\tau}{t_r}}} \end{aligned} \quad (6)$$

where $\mathcal{M}_\theta(\beta;\tau)$ and $\mathcal{M}_g(\beta)$ are the MTs in (3) of the auxiliary functions $\theta(\tau, a) = \chi^*(\tau, a)\sqrt{a}$ and $g(a) = x(at_r)$, respectively, and t_r is a normalization time ensuring that $(t-\tau)/t_r > 0$.

As noted in [?], if a signal $x(t)$ is localized in the time-frequency plane, it is also essentially limited in the Mellin domain. If we let the Mellin support of $g(a)$ to be such that $\mathcal{M}_g(\beta)$ is bounded within $\Theta = [-\beta_0/2, \beta_0/2]$, then we can replace $\mathcal{M}_g(\beta)$ in (6) with $P_{\beta_0}(\beta)\mathcal{M}_g(\beta)$, where $P_{\beta_0}(\beta) = 1$ for $\beta \in \Theta$ and zero otherwise.

After this replacement, the term $\mathcal{M}^*_\theta(\beta;\tau)P_{\beta_0}(\beta)$ in (6) can be expanded using a Fourier series

$$\mathcal{M}^*_\theta(\beta;\tau)P_{\beta_0}(\beta) = \sum_{m\in\mathbb{Z}} \tilde{\chi}(\tau, \mathrm{e}^{\frac{m}{\beta_0}})\mathrm{e}^{j2\pi m\frac{\beta}{\beta_0}} \qquad (7)$$

where $\tilde{\chi}(\tau, a)$ is a scale-smoothed version of $\chi(\tau, a)$

$$\tilde{\chi}(\tau, a) = \int_0^\infty \chi(\tau, a')\,\mathrm{sinc}\left(\beta_0(\ln a' - \ln a)\right) da' \qquad (8)$$

with $\mathrm{sinc}(x) = \sin(\pi x)/(\pi x)$.

Letting $\beta_0 = \frac{1}{\ln a_0}$, we can insert (7) into (6) to obtain,

$$y(t) = \sum_{m\in\mathbb{Z}} \int_{-\infty}^\infty \tilde{\chi}(\tau, a_0^m) a_0^{\frac{m}{2}} x(a_0^m(t-\tau))\, d\tau\,. \quad (9)$$

Note that the scale variable is geometrically sampled as $a = a_0^m, m \in \mathbb{Z}$, where $a_0 = \mathrm{e}^{\frac{1}{\beta_0}}$ is the basic scaling factor.

The procedure of discretizing the delay variable τ in (1) is entirely analogous to that of the scale variable. We first express the time convolution in (9) as the inverse Fourier transform of the frequency multiplication yielding

$$y(t) = \sum_{m\in\mathbb{Z}} \int_{-\infty}^\infty \tilde{U}(f\,; a_0^m) a_0^{-\frac{m}{2}} X(a_0^{-m} f)\, \mathrm{e}^{j2\pi f t} df \quad (10)$$

where $X(f)$ and $\tilde{U}(f\,; a_0^m)$ are the Fourier transforms of $x(\tau)$ and $\tilde{\chi}(\tau, a_0^m)$, respectively. If we assume that $X(f)$ is bandlimited to $[-\frac{W}{2}, \frac{W}{2}]$, then $a_0^{-\frac{m}{2}} X(a_0^{-m} f)$ is bandlimited to $[-\frac{a_0^m W}{2}, \frac{a_0^m W}{2}]$. Thus, $a_0^{-\frac{m}{2}} X(a_0^{-m} f)$ can be replaced by $P_{a_0^m W}(f) a_0^{-\frac{m}{2}} X(a_0^{-m} f)$ in (10), where $P_{f_0}(f) = 1$ for $-\frac{f_0}{2} \le f \le \frac{f_0}{2}$ and zero otherwise. Then, a Fourier expansion yields,

$$\tilde{U}(f\,; a_0^m) P_{a_0^m W}(f) = \sum_{n\in\mathbb{Z}} \hat{\chi}(\frac{n}{a_0^m W}, a_0^m)\mathrm{e}^{-j2\pi\frac{nf}{a_0^m W}} \quad (11)$$

where $\hat{\chi}(\tau, a_0^m)$ is a time-smoothed version of $\tilde{\chi}(\tau, a_0^m)$

$$\hat{\chi}(\tau, a_0^m) = \int_{-\infty}^{\infty} \tilde{\chi}(\tau', a_0^m)\,\mathrm{sinc}(a_0^m W(\tau - \tau'))d\tau' \,. \quad (12)$$

Substituting (11) into (10) and simplifying yields

$$y(t) = \sum_{m\in\mathbb{Z}}\sum_{n\in\mathbb{Z}} \hat{\chi}(\frac{n}{a_0^m W}, a_0^m)\, a_0^{\frac{m}{2}}\, x(a_0^m t - \frac{n}{W}) \,. \quad (13)$$

From (13), one can easily identify the time-scale sampling through the grid of $a = a_0^m$ and $\tau = n/(a_0^m W)$.

Note that a different, operator-based, wideband channel decomposition was obtained independently in [**?**], and a diversity application was discussed in [**?**].

3.3. Finite approximation

If the system of interest has bounded support $[A_0, A_1]$ in the scale domain, then (8) can be rewritten with $\beta = \frac{1}{\ln a_0}$ and a change of variable $a' = e^{\gamma}$ as

$$\tilde{\chi}(\tau, a_0^m) = \int_{\ln A_0}^{\ln A_1} \chi(\tau, e^{\gamma})\,\mathrm{sinc}\left(\frac{\gamma - m\ln a_0}{\ln a_0}\right) e^{\gamma} d\gamma \,. \; (14)$$

Considering the effective integration regions that overlap with the mainlobe of the sinc function in (14), the mth coefficient $\tilde{\chi}(\tau, a_0^m)$ in (9) is significantly nonzero only when $M_0 \le m \le M_1$, where[1] $M_0 = \lfloor \frac{\ln A_0}{\ln a_0} \rfloor$ and $M_1 = \lceil \frac{\ln A_1}{\ln a_0} \rceil$.

On the other hand, if $\chi(\tau, a)$ is bounded within $[0, T_m]$ in the time-delay domain, so is $\tilde{\chi}(\tau, a)$ in (8). As a result, the significant nonzero coefficients in (12)

$$\hat{\chi}(\frac{n}{a_0^m W}, a_0^m) = \int_0^{T_m} \tilde{\chi}(\tau', a_0^m)\,\mathrm{sinc}(n - a_0^m W\tau')d\tau'$$

correspond to $0 \le n \le N_m$, where $N_m = \lceil a_0^m W T_m \rceil$.

Combining both the discretization and the approximation, then $y(t)$ in (1) admits the following representation,

$$y(t) \approx \sum_{m=M_0}^{M_1}\sum_{n=0}^{N_m} \chi_{n,m}\, x_{n,m}(t) \quad (15)$$

where $\chi_{n,m} = \hat{\chi}(\frac{n}{a_0^m W}, a_0^m)$ is the discrete coefficient sampled from a two-dimensional smoothed version of $\chi(\tau, a)$

$$\begin{aligned}\hat{\chi}(\tau, a) &= \int_{A_0}^{A_1}\int_0^{T_m} \chi(\tau', a')\,\mathrm{sinc}(aW(\tau - \tau')) \\ &\quad \cdot \mathrm{sinc}\left(\frac{\ln a' - \ln a}{\ln a_0}\right) d\tau' da'\end{aligned}$$

and $x_{n,m}(t)$ is a time-scaled and shifted version of $x(t)$

$$x_{n,m}(t) = a_0^{\frac{m}{2}}\, x(a_0^m t - \frac{n}{W}) \,. \quad (16)$$

The truncated time-scale canonical model corresponding to (15) is demonstrated in Fig. 1.

[1] Note that $\lfloor x \rfloor$ ($\lceil x \rceil$) rounds x to the integer nearest to zero (infinity).

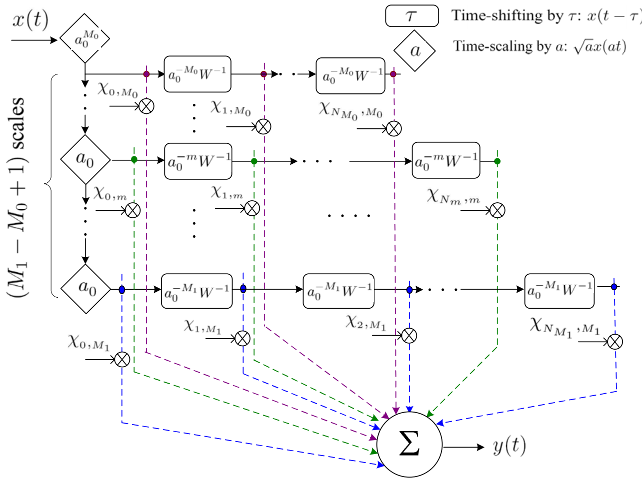

Fig. 1. Time-scale canonical model of a wideband system.

4. WIDEBAND MULTIPATH-SCALE DIVERSITY

4.1. Multipath-scale diversity and dyadic sampling

The wideband LTV system model is often matched to high speed underwater or high data rate wideband communications, where time-varying scattering and multipath propagation are subjected to fading degradations. One of the widely used methods to combat fading is diversity [?] that combines independently faded replicas of the transmitted signal at the receiver before demodulation and detection. As we will demonstrate next, the proposed canonical time-scale representation in (15) will provide the desired diversity when dyadic sampling and wavelet signaling are used.

When the wideband LTV system satisfies uncorrelated scattering as in (2), and if $\Omega(\tau, a)$ is sufficiently smooth, then we can show mutual uncorrelation over different discrete scales and delays [?],

$$E\left[\chi_{n,m}\,\chi^*_{n',m'}\right] \approx \Omega(\frac{n}{a_0^m W}, a_0^m)\, a_0^{2m}\, \delta[n - n']\delta[m - m'] \,.$$

When $\chi_{n,m}$ are Gaussian random variables, they are statistically independent. Hence, the time-scale canonical model with statistically independent coefficients provides

$$M = \sum_{m=M_0}^{M_1} (N_m + 1) \quad (17)$$

replicas of the transmitted signal, resulting in an inherent *joint multipath-scale* diversity of order M.

In order for a time-scale RAKE receiver to correctly combine the aforementioned diversity components, the basic waveforms $x_{n,m}(t)$ in (16) should be orthogonal. In [**?**], we proposed a wavelet-based waveform design which allows only dyadic scalings, i.e., $a = 2^m, m \in \mathbb{Z}$. Specifically, if we choose $x(t) = \frac{1}{\sqrt{T_s}}\psi(\frac{t}{T_s})$, where $\psi(t)$ is the scaling function of an orthonormal wavelet basis and $W \approx T_s^{-1}$, then for any $n, m, n', m' \in \mathbb{Z}$, $x_{n,m}(t)$ can be verified to satisfy the orthonormality condition

$$\int_{-\infty}^{\infty} x_{n,m}(t) x^*_{n',m'}(t)\, dt = \delta[n-n']\, \delta[m-m'] \,.$$

Note that $a_0 = 2$ in (13) ultimately leads to sampling the multipath-scale plane in a dyadic lattice as shown in Fig. 2 (a). Furthermore, this dyadic structure can be realized by choosing $\psi(t)$ as a Haar wavelet. The Haar wavelet $\psi(t)$ and its MT $\mathcal{M}_\psi(\beta)$ are plotted in Fig. 2 (b). As assumed in our derivation in Section 3.2, the support of the MT of $x(t) = \frac{1}{\sqrt{T_s}}\psi(\frac{t}{T_s})$ is essentially within $\beta \in [-\frac{1/2}{\ln 2}, \frac{1/2}{\ln 2}]$ as shown by the dotted region in Fig. 2 (b).

4.2. Simulation Results

In this section, we demonstrate the multipath-scale diversity gains that can be obtained for binary, antipodal signaling over three simulated wideband channels. The modulation waveform $x(t)$ with duration $T_s = 0.5$ ms was designed based on the Haar wavelet as discussed in Section 4.1, leading to dyadic channel decompositions. The channel parameters are specified in Table 1. All independent sub-channels have the same SNR. The channel coefficients are assumed to be Rayleigh fading and known at the receiver. The coherent detection of the time-scale RAKE receiver corresponds to a maximum ratio combining (MRC) and was discussed in [?]. The performance of the time-scale RAKE receiver is shown in Fig. 3 to increase for increasing M in (17). As it can be seen, the simulated results for $M = 5, 8$ and 10 follow the theoretical curves for Mth order diversity with MRC detection [?].

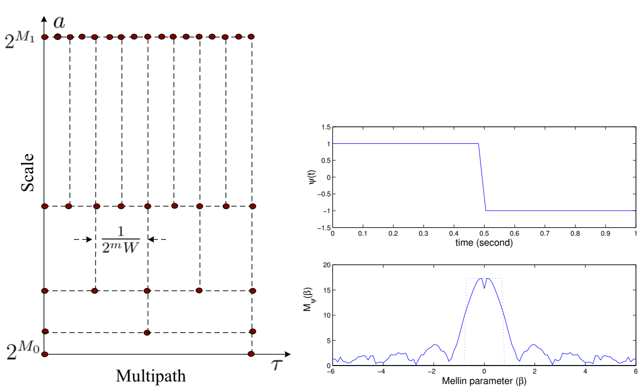

(a) (b)

Fig. 2. (a) Dyadic sampling. (b) Haar wavelet and its MT.

Channel	T_m	A_0	A_1	M_0	M_1	N_m	M in (17)
I	0.8 ms	0.6	0.8	-1	0	1, 2	5
II	0.8 ms	1.0	1.8	0	1	2, 4	8
III	0.8 ms	0.6	1.8	-1	1	1, 2, 4	10

Table 1. System parameters for three wideband channels.

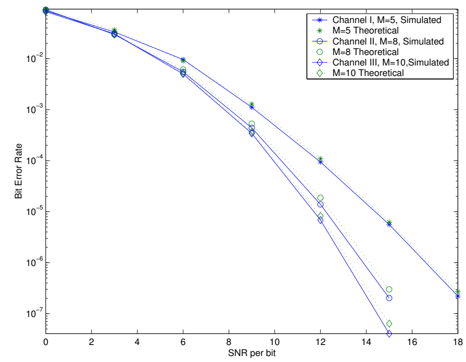

Fig. 3. Multipath-scale diversity.

5. CONCLUSION

We developed a time-scale canonical model to represent wideband LTV systems in terms of discrete Doppler scalings and time shifts, weighted by a smoothed WSF. This model was derived based on sampling the signal in the matched Mellin and Fourier domains. The important implication of this model is the multipath-scale diversity that is inherent to a wideband LTV communication channel with known Doppler scale and multipath spread. A signaling and reception scheme based on orthonormal wavelet basis is demonstrated to achieve the diversity gain effectively.

6. REFERENCES

[1] P. A. Bello, "Characterization of randomly time-variant linear channels," *IEEE Transactions on Communications*, vol. 11, May 1963.

[2] J. G. Proakis, *Digital Communications*, McGraw-Hall, Inc., 2001.

[3] A M. Sayeed and B. Aazhang, "Joint multipath-Doppler diversity in mobile wireless communications," *IEEE Transactions on Communications*, vol. 47, pp. 123–132, Jan. 1999.

[4] L. G. Weiss, R.K. Young, and L. H. Sibul, "Wideband processing of acoustic signals using wavelet transforms. Part I. Theory," *Journal of the Acoustic Society of America*, pp. 850–856, Aug. 1994.

[5] M. Stojanovic and L. Freitag, "Hypothesis-feedback equalization for direct-sequence spread-spectrum underwater communication," in *MTS/IEEE, Oceans*, Provience, RI, Sept. 2000, vol. 1, pp. 123–129.

[6] Y. Jiang and A. Papandreou-Suppappola, "Discrete time-scale canonical model for wideband LTV systems," *IEEE Transactions on Signal Processing*, Nov. 2004, submitted.

[7] J. Bertrand, P. Bertrand, and J. P. Ovarlez, "The Mellin transform," in *The Transforms and Applications Handbook*, A. D. Poularikas, Ed., chapter 11, pp. 829–885. CRC Press, 1996.

[8] L. Cohen, "The scale representation," *IEEE Transactions on Signal Processing*, vol. 41, no. 12, pp. 3275–3292, Dec. 1993.

[9] R. Balan, H. V. Poor, S. Rickard, and S. Verdu, "Time-frequency and time-scale canonical representations of doubly spread channels," in *Proceedings of European Signal Processing Conference*, Vienna, Austria, Sept. 2004.

[10] A. R. Margetts and P. Schniter, "Joint scale-lag diversity in mobile ultra-wideband systems," in *Proceedings of Asilomar Conference on Signals, Systems and Computers*, Pacific Grove, CA, Nov. 2004.

[11] Y. Jiang and A. Papandreou-Suppappola, "Characterization of wideband time-varying channels with multipath-scale diversity," in *Proceedings of IEEE Statistical Signal Processing Workshop*, St. Louis, MO, Sept. 2003, pp. 50–53.